Novel glucose sensor based on enzyme-immobilized 81° tilted fiber grating

Binbin Luo,[1,2,*] Zhijun Yan,[1] Zhongyuan Sun,[1] Jianfeng Li,[1] and Lin Zhang[1]

[1]*Aston Institute of Photonic Technologies, Aston University, Birmingham, B4 7ET, UK*
[2]*Department of Electronic Engineering, Chongqing University of Technology, Chongqing, 400054, China*
**luobinbin@cqut.edu.cn*

Abstract: We demonstrate a novel glucose sensor based on an optical fiber grating with an excessively tilted index fringe structure and its surface modified by glucose oxidase (GOD). The aminopropyltriethoxysilane (APTES) was utilized as binding site for the subsequent GOD immobilization. Confocal microscopy and fluorescence microscope were used to provide the assessment of the effectiveness in modifying the fiber surface. The resonance wavelength of the sensor exhibited red-shift after the binding of the APTES and GOD to the fiber surface and also in the glucose detection process. The red-shift of the resonance wavelength showed a good linear response to the glucose concentration with a sensitivity of 0.298nm·(mg/ml)$^{-1}$ in the very low concentration range of 0.0~3.0mg/ml. Compared to the previously reported glucose sensor based on the GOD-immobilized long period grating (LPG), the 81° tilted fiber grating (81°-TFG) based sensor has shown a lower thermal cross-talk effect, better linearity and higher Q-factor in sensing response. In addition, its sensitivity for glucose concentration can be further improved by increasing the grating length and/or choosing a higher-order cladding mode for detection. Potentially, the proposed techniques based on 81°-TFG can be developed as sensitive, label free and micro-structural sensors for applications in food safety, disease diagnosis, clinical analysis and environmental monitoring.

©2014 Optical Society of America

OCIS codes: (060.0060) Fiber optics and optical communications; (060.2370) Fiber optics sensors; (170.0170) Medical optics and biotechnology.

References and links

1. X. D. Wang and O. S. Wolfbeis, "Fiber-Optic chemical sensors and biosensors (2008-2012)," Anal. Chem. **85**(2), 487–508 (2013).
2. D. J. J. Hu, J. L. Lim, M. K. Park, L. T.-H. Kao, Y. Wang, H. Wei, and W. Tong, "Photonic crystal fiber-based interferometric biosensor for streptavidin and biotin detection," IEEE J. Sel. Top. Quantum Electron. **18**(4), 1293–1297 (2012).
3. S. M. Topliss, S. W. James, F. Davis, S. P. J. Higson, and R. P. Tatam, "Optical fibre long period grating based selective vapour sensing of volatile organic compounds," Sens. Actuators B Chem. **143**(2), 629–634 (2010).
4. S. D. Puckett and G. E. Pacey, "Detection of water in jet fuel using layer-by-layer thin film coated long period grating sensor," Talanta **78**(1), 300–304 (2009).
5. J. A. Barnes, R. S. Brown, A. H. Cheung, M. A. Dreher, G. Mackey, and H.-P. Loock, "Chemical sensing using a polymer coated long-period fiber grating interrogated by ring-down spectroscopy," Sens. Actuators B Chem. **148**(1), 221–226 (2010).
6. J. Kanka, "Design of turn-around-point long-period gratings in a photonic crystal fiber for refractometry of gases," Sens. Actuators B Chem. **182**, 16–24 (2013).
7. Y. F. Qi, X. Q. Gao, and W. H. Bi, "Refractive index biosensor based on microstructured optical fiber long-period gratings: a theoretical analysis," J. Opt. Soc. Am. B **30**(5), 1256–1260 (2013).
8. Y. Tian, W. H. Wang, N. Wu, X. T. Zou, and X. W. Wang, "Tapered optical fiber sensor for label-free detection of biomolecules," Sensors (Basel) **11**(4), 3780–3790 (2011).
9. H. Latifi, M. I. Ziba II, S. M. Hosseini, and P. Jorge, "Nonadiabatic tapered optical fiber for biosensor applications," Photonic Sensors **2**(4), 340–356 (2012).
10. W. H. Long, W. W. Zou, X. W. Li, and J. P. Chen, "DNA optical nanofibers: preparation and characterization," Opt. Express **20**(16), 18188–18193 (2012).

#224700 - $15.00 USD Received 9 Oct 2014; revised 12 Nov 2014; accepted 18 Nov 2014; published 1 Dec 2014

11. G. H. Wang, P. P. Shum, H. P. Ho, X. Yu, D. J. J. Hu, Y. P. Cui, L. M. Tong, and C. L. Lin, "Modeling and analysis of localized biosensing and index sensing by introducing effective phase shift in microfiber Bragg grating (μFBG)," Opt. Express **19**(9), 8930–8938 (2011).
12. Z. He, F. Tian, Y. Zhu, N. Lavlinskaia, and H. Du, "Long-period gratings in photonic crystal fiber as an optofluidic label-free biosensor," Biosens. Bioelectron. **26**(12), 4774–4778 (2011).
13. X. Chen, L. Zhang, K. Zhou, E. Davies, K. Sugden, I. Bennion, M. Hughes, and A. Hine, "Real-time detection of DNA interactions with long-period fiber-grating-based biosensor," Opt. Lett. **32**(17), 2541–2543 (2007).
14. H. S. Jang, K. N. Park, J. P. Kim, S. J. Sim, O. J. Kwon, Y.-G. Han, and K. S. Lee, "Sensitive DNA biosensor based on a long-period grating formed on the side-polished fiber surface," Opt. Express **17**(5), 3855–3860 (2009).
15. S. M. Tripathi, W. J. Bock, P. Mikulic, R. Chinnappan, A. Ng, M. Tolba, and M. Zourob, "Long period grating based biosensor for the detection of escherichia coli bacteria," Biosens. Bioelectron. **35**(1), 308–312 (2012).
16. C. L. Eggen, Y. S. Lin, T. Wei, and H. Xiao, "Detection of lipid bilayer membranes formed on silica fibers by double-long period fiber grating laser refractometry," Sens. Actuators B Chem. **150**(2), 734–741 (2010).
17. T. M. Libish, J. Linesh, M. C. Bobby, B. Nithyaja, S. Mathew, C. Pradeep, and P. Radhakrishnan, "Glucose concentration sensor based on long period grating fabricated from hydrogen loaded photosensitive fiber," Sensors and Transducers Journal **129**(6), 142–148 (2011).
18. D. W. Kim, Y. Zhang, K. L. Cooper, and A. Wang, "In-fiber reflection mode interferometer based on a long-period grating for external refractive-index measurement," Appl. Opt. **44**(26), 5368–5373 (2005).
19. A. Deep, U. Tiwari, P. Kumar, V. Mishra, S. C. Jain, N. Singh, P. Kapur, and L. M. Bharadwaj, "Immobilization of enzyme on long period grating fibers for sensitive glucose detection," Biosens. Bioelectron. **33**(1), 190–195 (2012).
20. K. Zhou, L. Zhang, X. Chen, and I. Bennion, "Optic sensors of high refractive-index responsivity and low thermal cross sensitivity that use fiber Bragg gratings of >80 ° tilted structures," Opt. Lett. **31**(9), 1193–1195 (2006).
21. X. W. Shu, L. Zhang, and I. Bennion, "Sensitivity characteristics of long-period fiber gratings," J. Lightwave Technol. **20**(2), 255–266 (2002).

1. Introduction

Optical fiber biosensors have been proved as good tools for detecting specific bio-molecules in the fields of food safety, drug discovery, medical diagnosis and environmental monitoring [1–4], due to their advantages of small size, label free and high sensitivity and good selectivity. So far, many interests have been focused on the biosensors based on the long period gratings (LPGs) [5] and their combination with photonic crystal fiber (PCF) [6] or microstructure optical fiber (MOF) [7], or based on the tapered fiber [8,9], micro/nano fiber [10] and microfiber Bragg grating [11]. With their surface functionalized by molecular recognition elements (i.e., antibodies, enzyme, etc.), the biosensors mentioned above have been reported for the detection of antigen [8, 12], DNA [10, 13, 14], escherichia coli bacteria [15], and medically relevant parameters [16].

In clinic examination, it is very important to test the concentration of blood glucose, as glucose is the key source of energy of human body, through aerobic respiration, providing about 3.75 kilocalories of food energy per gram. A normal person's blood glucose concentration is in the range of 0.10~3.0 mg/mL, and for a healthy person is 0.7~1.1mg/mL. Presently, only electrochemical methods are more popular for the glucose analysis. In some published papers, unmodified LPG sensors have been used for non-selective analysis of very highly concentrated glucose solutions, e.g. 300mg/mL [17, 18]. Recently, Akash Deep [19] has proposed an enzyme-modified standard LPG as the selective method for glucose detection. Due to the conversion of the glucose to the gluconic acid under the catalytic reaction of a fungal enzyme, this selective method can detect the glucose concentration as low as 0.10~3.0mg/mL, corresponding to that of the physiological range, and can provide a fast response online test for glucose. Although the LPG sensor is simple to fabricate, but it suffers from the thermal and tensile cross-talk effect, because of its inherent properties of highly sensitive to the temperature and strain, and also its Q-factor is relatively low due to broad resonant spectrum.

We report in this paper for the first time to modify the surface of an 81° tilted fiber grating (81°-TFG) for a cost-effective, high accuracy (i.e., high Q-factor), ultra stable, label-free specific detection of glucose. The 81°-TFG based glucose sensor showed much lower thermal cross-talk effect, higher refractive index (RI) sensitivity, better linearity and higher Q-factor than the previously reported enzyme-immobilized LPG based sensor [19]. Theoretically

#224700 - $15.00 USD Received 9 Oct 2014; revised 12 Nov 2014; accepted 18 Nov 2014; published 1 Dec 2014
(C) 2014 OSA

speaking, its sensitivity to the glucose concentration can be further improved by increasing the grating length and/or choosing a higher-order cladding mode for detection.

2. Fabrication and properties of 81°-TFG

2.1 Fabrication of 81°-TFG

The 81°-TFGs were UV inscribed in H_2-loaded SM-28 fiber by using scanning mask technique. We used a custom-designed amplitude mask with a period of 6.6μm, which ensures that the grating response generated from high order cladding modes coupling is centered in the C-L band. In the UV-inscription, the amplitude mask was tilted at 78°, thus producing excessively tilted fringes at ~81° in the fiber core. Figure 1(a) shows a micrograph of the 81°-TFG, displaying the tilted fringes occupying all fiber core area with a grating period of ~32μm and tilted angle of 81.07°. The excessively tilted fringes in the fiber core will couple the light from the core mode to the co-propagating high-order cladding modes, thus such a TFG with large tilted angle may be regarded as an LPG with much smaller grating period, as shown in Fig. 1(b). The 81°-TFG is inherently very sensitive to the surrounding medium refractive index and can be implemented as an optical fiber biosensor platform [20].

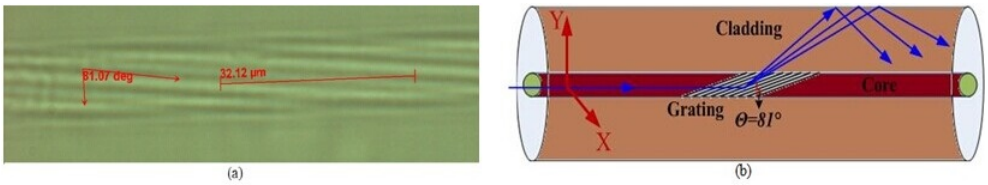

Fig. 1. (a) Micrograph of the fiber core and (b) mode coupling of the 81°-TFG.

2.2 Properties of 81°-TFG

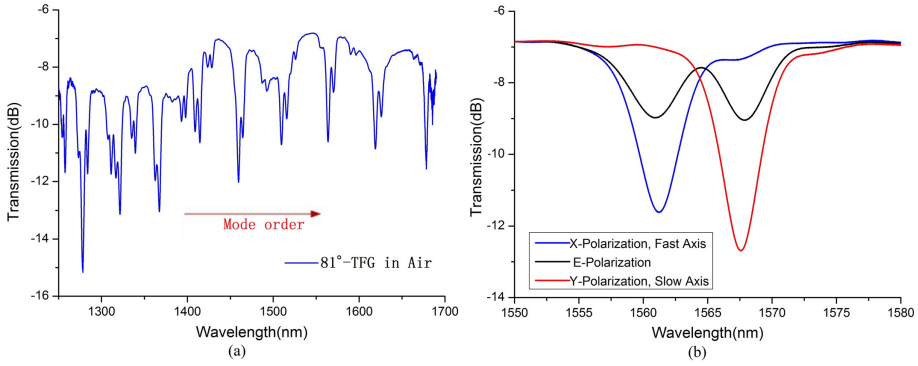

Fig. 2. (a) 81°-TFG spectrum in 1250~1700nm with un-polarized probe light and (b) its zoomed spectra for one pair of dual-peaks with X- and Y-polarized and un-polarized light.

Since the grating period (~32μm) of 81°-TFG is much smaller than that (~550μm) of standard LPG, the separations of its coupled cladding modes are much closer. Figure 2(a) shows the measured transmission spectrum of an 81°-TFG from 1250nm to 1700nm when it was probed with an un-polarized light. It can be seen from the figure that the separation of adjacent cladding modes increases from ~40nm to ~70nm with increasing mode order. More pronouncedly, we see the dual-peak feature of the resonance in the figure. Obviously, the excessively tilted fringes can induce a significant birefringence in the fiber core, resulting in dual-peak resonances that correspond to the two orthogonal polarization modes. Figure 2(b) shows a zoomed plot for one pair of dual-peaks centered around 1550nm to 1580nm: the blue curve shows the fast-axis mode fully excited when the grating is probed with X-polarization light, whereas the red curve indicates the slow-axis mode fully coupled when probed with Y-

#224700 - $15.00 USD Received 9 Oct 2014; revised 12 Nov 2014; accepted 18 Nov 2014; published 1 Dec 2014
(C) 2014 OSA

polarization light; the black curve shows the spectrum when probed with un-polarized light exhibiting two equally coupled modes of ~3dB strength.

The resonant condition of the 81°-TFG can be expressed as

$$\lambda_c^{x,y} = (n_{co}^{x,y} - n_{cl}^{m}) \cdot \Lambda. \quad (1)$$

where $\lambda_c^{x,y}$ is the resonant wavelength for X- or Y-polarization, $n_{co}^{x,y}$ and n_{cl}^{m} are the effective indexes of the fiber core in fast- (X) or slow-axis (Y) and the m^{th}-order cladding mode, respectively, and Λ is the grating period. Due to the refractive index of the fast-axis is slightly lower than that of the slow-axis, the two peaks will response differently to the surrounding medium condition. According to our experimental results, the RI sensitivities of the X-polarized and Y-polarized modes at ~1560nm region are ~168.0nm/RIU and ~158.0nm/RIU in the RI range of 1.333~1.370, repetitively, as shown in Fig. 3(a), which are higher than that of normal LPG. Their temperature sensitivities are ~5.30pm/°C and ~4.95pm/°C, respectively, as shown in Fig. 3(b), which are significantly lower than that of the LPG and FBG. In order to gain a relatively higher sensitivity to the RI with a low temperature cross-talk effect, we have only excited the X-polarized mode in the glucose detection experiment described below.

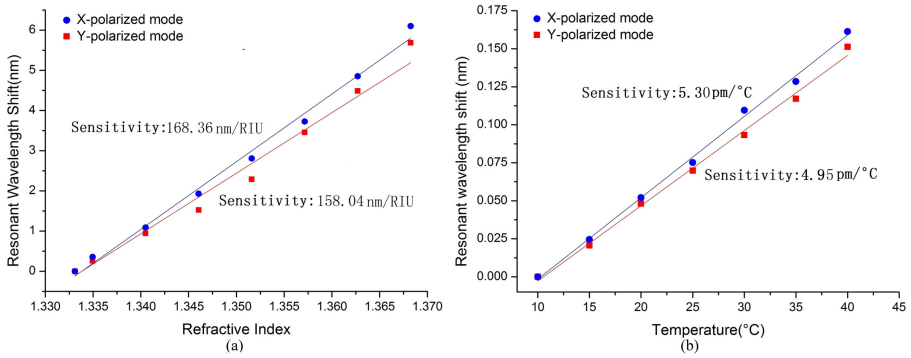

Fig. 3. Measured (a) RI and (b) temperature sensitivity of the 81°-TFG.

3. Surface modification for 81°-TFG and glucose detection

3.1 Surface modification for 81°- TFG sensor

In order to achieve the selective method for glucose detection, the fiber surface of the grating sensor should be bio-functionalized by the GOD firstly [19]. The 81°-TFG was initially immersed in HNO_3 solution (5% v/v) for ~2h at ~40°C to remove the contamination and then thoroughly washed by de-ionized water and ethanol. The cleaned fiber was then immersed in the H_2SO_4 solution (95% v/v in H_2O_2) for ~1h at room temperature to activate the hydroxyl-groups (i.e., '-OH') on the glass surface followed by drying under an incandescent lamp for ~18h at ~40°C. It has been known that aminopropyltriethoxysilane(APTES) has an positive charge with NH^{3+} in the side chain and can be used for adsorbing bio-molecules with negative charge like escherichia coli bacteria and glucose oxidase (GOD) [15, 19]. Hence we used an APTES solution (10% v/v in ethanolic solution) to incubate the -OH activated fiber for ~40 min at room temperature in the silanized process, in which the NH^{3+} groups of the APTES molecules would covalently link to the -OH groups of the glass surface. Afterwards, the fiber was washed by de-ionized water and ethanol to remove non-covalently bonded silane compounds. Finally, the immobilization of enzyme molecules on the fiber surface was realized by immersed the silane fiber in 10mg/ml sodium acetate (SA) buffered solution of GOD for 2h incubation, in which the GOD's -COOH groups would bind with the NH^{3+} groups on the surface of the silane fiber through covalent interaction. Subsequently, the

#224700 - $15.00 USD Received 9 Oct 2014; revised 12 Nov 2014; accepted 18 Nov 2014; published 1 Dec 2014
(C) 2014 OSA

enzyme-immobilized fiber was washed with SA buffer and de-ionized water again and dried in the air. Figure 4 depicts the whole process of the fiber surface modification.

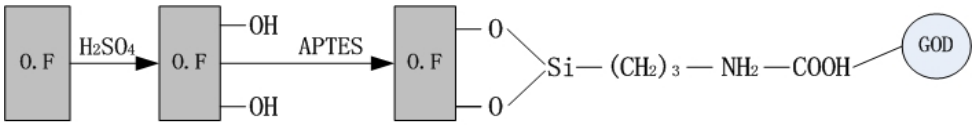

Fig. 4. Modified process for the fiber surface of the 81°-TFG.

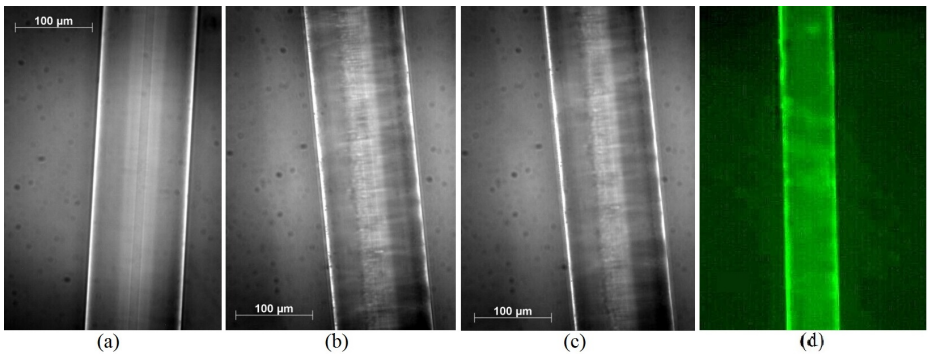

Fig. 5. Micro image of the (a) Cleaned fiber (b) Silane fiber (c) GOD-immobilized fiber (d) fluorescence fiber.

After the surface modification experiment, the GOD-immobilized fiber was examined under microscope. Figures 5(a)-5(c) show the micro images of the 81°-TFG observed by confocal microscopy (40 ×) after cleaning, silanization and GOD-immobilization process, respectively. The comparison of Figs. 5(a) and 5(b) clearly shows that the surface of grating has been covered by a smooth silane layer. However, comparing Figs. 5(b) with 5(c), there are no obvious differences between them. In order to verify the GOD molecules having been immobilized on the fiber surface, intrinsic fluorescent property of GOD was utilized. A fluorescent microscope (20 ×) with white light source was used for excitation. Figure 5(d) shows the strong glowing fluorescence, indicating sufficient GOD molecules have been immobilized on the surface of the 81°-TFG.

Apart from the microscope inspection to evaluate the effectiveness of GOD-immobilization, the spectrum evolution of the immobilized 81°-TFG was monitored *in situ* throughout the modification process. Figure 6(a) shows the spectra of X-polarized mode and the corresponding central wavelength of the peak for the cleaned, silanized and GOD-immobilized 81°-TFG as immersing in the SA buffered solutions. We can clearly see that the initial resonant wavelength has undergone a red-shift as a consequence of the adsorption of additional layers on the fiber surface and hence gradually changing the n_{cl}^{m} . The silanization has induced a relatively small red-shift of 0.2nm whereas the GOD-immobilization has moved the central peak by 0.6nm. This can be explained by the fact that the molecular weight (156,000) of GOD is much larger than that (221.37) of the APTES, thus resulting in a relatively remarkable effect on n_{cl}^{m} .

#224700 - $15.00 USD Received 9 Oct 2014; revised 12 Nov 2014; accepted 18 Nov 2014; published 1 Dec 2014
(C) 2014 OSA

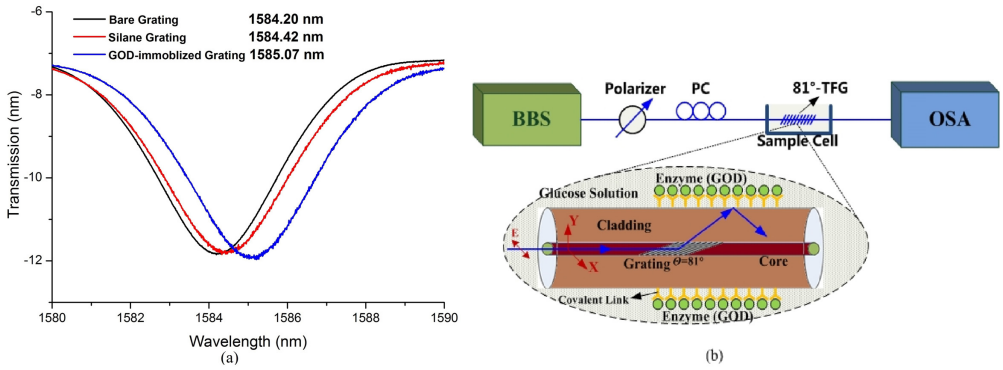

Fig. 6. (a) Spectra and resonant wavelengths of the 81°-TFG after cleaning, silanization and GOD-immobilization process, (b) Experimental setup for investigating the correlation between D-Glucose concentration and grating spectral response.

3.2 Glucose detection by selective method

The prepared GOD-immobilized 81°-TFG sensor was used for glucose detection. The selective method for glucose detection is based on the principle that the specific enzyme (i.e., GOD) immobilized on the surface of the 81°-TFG will cause the glucose (molecular weight = 180.6) to convert to the gluconic acid (molecular weight = 192.6), as shown in Eq. (2), leading to a relatively large RI change even in a dilute (e.g. 0.1~3mg/mL) glucose solution, which will in turn, cause a detectable shift of the resonance wavelength of the grating sensor.

$$D\text{-}Glu\cos e + H_2O + O_2 \xrightarrow{GOD} D\text{-}Gluconic \quad acid + H_2O_2. \tag{2}$$

GOD used in our experiment was purchased from Sigma, and its enzymatic activity is larger than 200units/mg and one unit GOD will oxidize 1.0μmole of β-D-Glucose to D-Gluconic acid and H_2O_2 per minute at pH ~5.1 at 35°C. Therefore, we prepared different concentrations of D-Glucose (0.1, 0.5, 1.0, 1.5, 2.0, 2.5, 3.0, 3.5, 4.0, 4.5, 5.0mg/ml) in the SA buffered solution (PH 5.2), which will provide a suitable chemical environment for this catalytic reaction. These SA buffer solutions of D-Glucose were kept for ~6h at room temperature to achieve an equilibrium status (containing two-third β-D-Glucose and one-third α-D-Glucose) before the test.

The experimental setup to investigate the correlation between D-Glucose concentration and grating spectral response is shown in Fig. 6(b). Light from a broadband source (BBS, 1550A-TS, 1495~1595nm) was launched into the fiber and the transmission spectrum was recorded by an optical spectrum analyzer (OSA, AQ-6370B) with a resolution of 0.02nm. A polarizer and a polarization controller (PC) were placed between the BBS and the grating to adjust and maintain the 81°-TFG to work only in the X-polarized mode.

At the beginning, a pure SA buffer solution was introduced in the sample cell, and the observed resonant wavelength of the 81°-TFG was recorded as the reference. Then the prepared SA buffered solutions of D-Glucose with different concentrations were introduced into the sample cell in turn to investigate the correlation between the D-Glucose concentration and the grating spectral response. In each test, we used a culture dish to cover the liquid sample to minimize its evaporation, since which could also change the RI of the liquid sample, leading the resonance spectrum to red shift. After each test, the de-ionized water was used to wash the grating to guarantee its resonant wavelength moving back to the reference point. By doing these, a stable resonance spectrum was recorded after 0.5-2min of the chemical reaction. For comparison, a non-modified 81°-TFG was also subjected to the evaluation.

Figure 7(a) is the evolution of the resonance spectrum (FWHM ~4.5 nm) with the increase of the glucose concentration from 0 to 3.0mg/ml. Because the red-shifted resonance amplitude is related to the change of average RI within the evanescence-field area

#224700 - $15.00 USD Received 9 Oct 2014; revised 12 Nov 2014; accepted 18 Nov 2014; published 1 Dec 2014
(C) 2014 OSA

surrounding the grating surface, therefore, according to Eq. (1) and Eq. (2), the more β-D-Glucose molecules (i.e., the higher the glucose solution concentration) and enough active GOD molecules exist in this evanescence-field area, the greater change of n_{cl}^{m} that affected by the change of this average RI will be. This will then result in a greater red-shift in the resonant wavelength. Figure 7(b) plots the resonant wavelength shift with D-Glucose concentration for the non-modified (square dots) and GOD-immobilized (circle dots) 81°-TFGs, indicating that, for the non-modified 81°-TFG, the resonant wavelength remains almost unchanged as the maximum variation of which is only ~0.08nm, compared with the reference point, while for the GOD-immobilized one, it is red-shift for 0.91nm and has a good linear response with the increase of the glucose concentration from 0 to 3.0mg/ml. Linear fitting shows that the detecting sensitivity for the glucose concentration is 0.298nm·(mg/ml)$^{-1}$ and the R-square ~0.99. The Q-factor of the sensor, defined by the working wavelength versus FWHM, is estimated to be ~1585nm/~4.5nm ≅ 352. However, the sensors did not respond properly in a higher concentration range from 3.0mg/ml to 5.0mg/ml. This may be due to the fact that since the activated grating length is only 10mm, above 3.0mg/ml, there were not enough active GODs to support a complete oxidation of the glucose molecules in this case, leading to a gradual decrease in the red-shifted amplitude of the resonant wavelength.

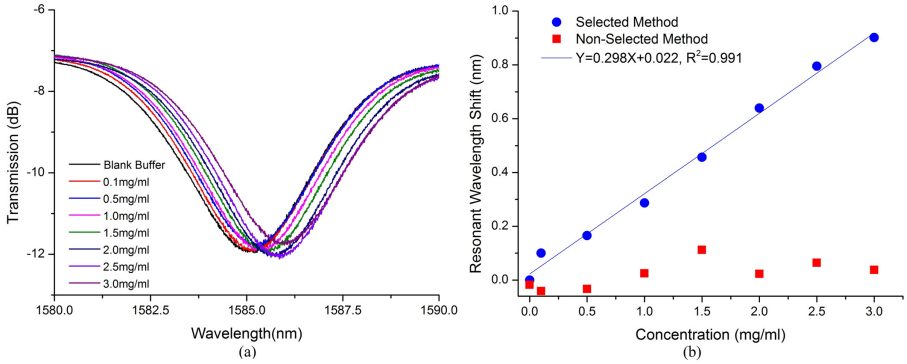

Fig. 7. (a) Spectrum evolution of 81°-TFG with the glucose concentration, (b) Shift of the resonant wavelength of 81°-TFG by the selective method and non-selective method in the concentration range of 0~3.0mg/ml.

In order to evaluate the sensor re-usability, the GOD and silane layers on the fiber grating surface were removed by using the HNO_3 solution. Then, the above described experiment was conducted again on the grating for three times, and the observed average variation in the resonant wavelength shift was only ~ ± 0.04nm, indicating a good reproducibility for the 81°-TFG based biosensors.

For more specific comparison with LPG sensing performance, Table 1 gives the sensing parameters of the previously reported LPG (standard, Λ = ~550μm) based glucose sensor [19] and the 81°-TFG based one. For the standard LPG (period around 550μm) based glucose sensor [19], the order of cladding mode (at ~1550nm) hired for measurement is 4th or 5th [21], while for the 81°-TFG (period around 32μm) based one, the order of cladding mode (at ~1560nm) used for the test is calculated to be 35th, which is much higher than the one of LPG. It can be seen clearly from the table that the intrinsic properties of the latter is much better than that of the former, because it induces much lower thermal cross effect and higher RI sensitivity. Particularly, the latter has a much narrower bandwidth leading to ~4.5 times improvement in Q-factor than that of the former. However, two important parameters (i.e., red-shift amplitude and glucose detection sensitivity) of the latter are smaller than that of the former. This can properly be explained by the fact that these two parameters are determined by the quantity of the GOD molecules immobilized on the grating surface, which is closely related to the grating length and the surface modification effect. Knowing that the length of

#224700 - $15.00 USD Received 9 Oct 2014; revised 12 Nov 2014; accepted 18 Nov 2014; published 1 Dec 2014
(C) 2014 OSA

this 81°-TFG we used is only half of that of the previously reported LPG, thus the change of the average RI within the evanescence-field area of the 81°-TFG surface is not as large as that in the case of LPG based sensor. Therefore, theoretically speaking, we can fabricate and bio-functionalize a longer 81°-TFG to increase the effective quantity of the GOD molecules to improve its glucose detection sensitivity and the red-shift amplitude. In addition, choosing a relatively higher-order cladding mode of 81°-TFG can further enhance these two parameters for biosensing performance, as the RI sensitivity of a higher-order mode of the 81°-TFG is larger than that of a lower-order one [20].

Table 1. Comparison of the Sensing Parameters between LPG based and 81°-TFG based Glucose Sensor

	Length /mm	| Tem. Sens. | /pm·°C^{-1}	RI Sens. /nm·RIU^{-1}	FWHM /nm	Q-factor	Meas. Range /mg·ml^{-1}	Red-shift amplitude /nm	Glu. Det. Sens. /nm·(mg/ml)$^{-1}$	R^2	Variation /nm
LPG	20	~300	−50~-100	~20	~80	0.1~3.0	~2.30	0.806	0.92	± 0.10
81°-TFG	10	~5.30	~168	~4.5	~352	0.0~3.0	~0.91	0.298	0.99	± 0.04

4. Conclusions

We have demonstrated a cost-effective biosensor based on an 81°-TFG to detect the glucose concentration within the physiological range (0~3.0mg/ml) of human being. The 81°-TFG is easy to fabricate, and the GOD immobilization has been achieved by modifying the grating surface with APTES. Comparing with the previous enzyme-immobilized LPG biosensor, the glucose sensor we proposed possesses several intrinsic advantages, including relatively higher RI sensitivity (~168nm/RIU), much lower thermal cross-talk effect and higher Q-factor (~352). The 81°-TFG based biosensor has also exhibited a better linearity (~0.99), much higher measurement accuracy and good stability for the detection of glucose solution even with extremely low concentration. As discussed, its detection sensitivity for glucose concentration can be further improved by increasing the grating length and/or choosing a relatively higher-order cladding mode for sensing. Combining all these advantages, the proposed 81°-TFG based biosensor could be a good alternative to be applied in various application fields such as disease diagnosis, microbial pathogen detection, life science (e.g., DNA hybridization monitoring), food safety control and environmental monitoring.

Acknowledgments

This paper was supported by the Research Fund from the National Natural Science Foundation of China under project 51276209 and 50876120, Natural Science Foundation Project of Chongqing City under cstc2014jcyjA0081, Education committee Project of Chongqing City under KJ130828, and Aston Institute of Photonic Technology Visitor Support.

#224700 - $15.00 USD Received 9 Oct 2014; revised 12 Nov 2014; accepted 18 Nov 2014; published 1 Dec 2014
(C) 2014 OSA